EFDA–JET–CP(14)06/07

C. Bourdelle, L. Chôné, N. Fedorczak, X. Garbet, P. Beyer, J. Citrin,
G. Dif-Pradalier, G. Fuhr, A. Loarte, C. Maggi, F. Militello, Y. Sarazin
and JET EFDA contributors

L to H Mode Transition: Parametric Dependencies of the Temperature Threshold by a Simple First Principles Approach

L to H Mode Transition: Parametric Dependencies of the Temperature Threshold by a Simple First Principles Approach

C. Bourdelle[1], L. Chôné[1], N. Fedorczak[1], X. Garbet[1], P. Beyer[2], J. Citrin[3], G. Dif-Pradalier[1], G. Fuhr[2], A. Loarte[4], C. Maggi[5], F. Militello[6], Y. Sarazin[1] and JET EFDA contributors*

JET-EFDA, Culham Science Centre, OX14 3DB, Abingdon, UK

[1]CEA, IRFM, F-13108 Saint-Paul-lez-Durance, France.
[2]Aix–Marseille Université, CNRS, PIIM UMR 7345, 13397 Marseille Cedex 20, France
[3]FOM Institute DIFFER–Dutch Institute for Fundamental Energy Research, PO Box 1207, 3430 BE Nieuwegein, The Netherlands
[4]ITER Organization, Route de Vinon sur Verdon, 13115 St Paul Lez Durance, France
[5]Max Planck Institut fur Plasmaphysik, EURATOM Association, Garching, Germany
[6]Culham Centre for Fusion Energy, Abingdon, UK
** See annex of F. Romanelli et al, "Overview of JET Results", (25th IAEA Fusion Energy Conference, St Petersburg, Russia (2014)).*

Preprint of Paper to be submitted for publication in Proceedings of the 25th IAEA Fusion Energy Conference, St Petersburg, Russia 13th October 2014 - 18th October 2014

ABSTRACT

The L to H mode transition happens for a critical power which, itself, depends on various parameters, such as the magnetic field, the density, etc. Experimental evidence on various tokamaks (JET, ASDEX-Upgrade, DIII-D, Alcator C-Mod) point towards the existence of a critical temperature characterizing the transition. This criterion for the L-H transition is local and is therefore easier to be compared to theoretical approaches. In order to shed light on the mechanisms of the transition, simple theoretical ideas are used to derive a temperature threshold (T_{th}). The obtained parametric dependencies of the derived T_{th} are tested versus magnetic field, density, effective charge. Various robust experimental observations are reproduced, in particular T_{th} increases with magnetic field B and increases very sharply with lower density below the density roll over observed on the power threshold.

1. INTRODUCTION

The L to H mode transition happens for a critical power which, itself, depends on various parameters, such as the magnetic field, the density, etc [1,2,3]. This global approach of the transition is difficult to compare to theoretical approaches based on local mechanisms. Therefore, various attempts to define the L to H transition in terms of local parameters have been carried out. The most recent was done on 67 JET pulses using a neural network classification technique [4]. A critical electron temperature increasing with large magnetic field B, decreasing with larger density n and weakly decreasing with safety factor q is reported.

In order to shed light on the transition mechanisms simple theoretical ideas are proposed. The only novelty being here the combination of two popular ideas [5]: the role of the L mode edge unstable Resistive Ballooning Modes [6] and the other characterizing the mean flow EB shear [7]. The principle is to identify two times, one characterizing the turbulence and one characterizing the mean flow. The assumption made is that the transition to H mode occurs when the shortest of the two times is the one characterizing the mean flow. RBM have been recently found to be linearly unstable in gyrokinetic modeling of JET-ILW pedestal forming region parameters [8]. The presence of unstable RBM has been shown to be in qualitative agreement with a larger power threshold obtained at larger Z_{eff}, see [8,9]. On the other hand, recent experimental measurements still point strongly towards a key role of E_r [10].

In sections 2 and 3, the choice for the turbulence growth is justified and derived; then the analytical derivation of the $E \times B$ shear is detailed. In section 4, the ratio of both times will be studied, and temperature threshold dependencies analyzed. In particular, the temperature threshold dependencies on B, n, Z_{eff}, the isotopic effect and He versus D are presented. It will be demonstrated that the stabilization trends are in qualitative agreement with the reported experimental tendencies. Finally, the weaknesses and strengths of the approach will be discussed before concluding in section 5.

2. THE TURBULENCE TIME SCALE: $1/\gamma_{\mathbf{turb}}$

Recent observations of the impact of the ITER-like-wall (ILW) in JET show a L to H mode power threshold reduced by $\simeq 40\%$ with respect to similar experiments in C wall [9]. A similar trend is reported in ASDEX Upgrade [11]. A common feature of both JET and ASDEX Upgrade is a significant reduction of Z_{eff} when switching from C walls to metallic ones. The link between a modified plasma shape and a modified Z_{eff} has been tested in JET-ILW by varying the upper and lower triangularities. A reduction of P_{th} (from 3 MW down to 1.5 MW) at constant density is observed to correlate better with a reduction of Z_{eff}, rather than with modified triangularity [8,9].

Based on JET-ILW data prior to the L to H mode transition, a linear gyrokinetic stability analysis has been performed with GENE [12] as reported in [8]. The temperature was scanned. At low temperature, corresponding to the temperature range where the transition is obtained, Resistive Ballooning Modes are found linearly unstable. Therefore, in the following, an analytical model is built to reproduce the competition between the stabilized RBM and the destabilized ITG-TEM as the temperature is increased.

The analytical derivation of the RBM growth rate is based on [13]. The dispersion relation accounts for ions and electrons, and allow to obtain both w_{RBM}, characterizing the eigenfunction width, and the growth rate, γ_{RBM}, characterizing the eigenvalue. In the following expressions, T_i and T_e can be different and $n_e = \sum_s Z_s n_s$. Moreover, the magnetic shear s and the MHD α contributions to the curvature and grad-B drifts are included. One then obtains:

$$\frac{\gamma_{RBM}}{\gamma_I} \simeq (\tau \bar{Z}_a)^{1/3}(1+\tau/\bar{Z})^{2/3}\,(k_\theta \rho)^{4/3}\left(\frac{6\gamma_I \nu}{\omega_{te}^2}\right)^{1/3} \tag{1}$$

with $\tau = T_i/T_e$, $\bar{Z} = \frac{n_e}{\sum_s n_s}$, $\rho = \frac{\sqrt{T_e m_D}}{eB} = \rho_D/\sqrt{2\tau}$, $\bar{Z}_a = \frac{n_e}{\sum_s A_s n_s}$ and $\omega_{te} = \dot{k_\parallel}\rho_D v_{the}$ the electron transit frequency (v_{the} the electron thermal velocity). $\gamma_I = \frac{c_s}{\sqrt{RL_p}}\sqrt{0.2(1+1.9(s-\alpha))}$ is the interchange growth rate. The curvature and grad-B drift for deeply trapped particles is averaged over the pitch angle leading to $\omega_g = \frac{k_\theta T_e}{eB}\frac{1}{R}0.2(1+1.9(s-\alpha))$. $c_s = \sqrt{T_e/m_D}$ is a thermal velocity. Note that, if $(1+1.9(s-\alpha)) < 0$ then γ_I is forced to zero as in such case there is no drive for the interchange instability.

From equation 1, it is clear that RBM are destabilized if the product of the interchange growth rate with the collisionality, $\gamma_I \nu$, is large compared to the square of the electron parallel transit frequency, ω_{te}^2.

As the temperature is increased RBM are stabilized and ITG-TEM take over. To account for this competition, an analytical model for ITG-TEM is proposed. The gyrokinetic equation is developed in the limit where the frequency of the unstable modes is much larger than drift frequencies, also called fluid limit. The passing electrons are assumed adiabatic. The finite Larmor radius effect are taken in the low wave number limit. The lowest order ballooning representation is used. Details of this derivation are given in the appendix D of [14]. In the absence of rotation, and after integrating over energy and pitch angle, one obtains:

$$\gamma_{ITG-TEM} = (k_\theta \rho_i)^2 \gamma_I \frac{1}{1-f_t}\sqrt{\left(f_t + \frac{\tau}{\bar{Z}}\right)^2 - \left(0.07 f_t \frac{\nu}{n\bar{\omega}_{de}}\right)^2} \tag{2}$$

The factor 0.07 has been set to match a temperature scan done with GENE as illustrated by figures 1 and 2. In the case of $\left(f_t + \frac{\tau}{\bar{Z}}\right)^2 < \left(0.07 f_t \frac{\nu}{n\bar{\omega}_{de}}\right)$, ITG only are unstable.

A growth rate for the RBM branch and one for the ITG-TEM branch have been derived analytically. The way they compete over a temperature scan for $k_\theta \rho_i = 0.1$ is studied for a set of parameters inspired by a JET-ILW pulse prior to the transition into H mode [8]. $k_\theta \rho_i = 0.1$ is chosen since low k_θ modes typically have the highest weight in the transport flux spectrum. The density is varied to two other lower values: $0.4 \times 10^{19} m^{-3}$ and $1 \times 10^{19} m^{-3}$. If the density is decreased, the collisionality decreases leading to weaker RBM and stronger TEM contribution to the ITG-TEM branch [15]. This is what is reported in figure 1 for GENE and on figure 2 for the analytical model. The fluid model leads to a minimum growth rate at a temperature similar

to the GENE calculation. On the ITG-TEM branch, as the density is increased, the collisionality is larger and the TEM are lower leading to lower growth rates. On the RBM branch, as the density is increased the modes are destabilized by larger collisionality. The analytical growth rates are larger than the computed ones with GENE. Indeed, the fluid limit is known to overestimate the growth rates. It is interesting to note that the stabilization of these interchange modes by the α parameter occurs at temperatures 3 to 10 times larger than the experimentally reported values, whereas the RBM stabilization occurs at T in the experimental range see figure 1.

3. THE MEAN FLOW TIME SCALE: $1/\gamma_E$

The electric field E_r is estimated at two radial locations. One at the last closed flux surface, where E_r is known to scale with ∇T_e [16]. Therefore, assuming a temperature profile having a fixed gradient length L_T, one gets: $E_r(1) = 3\frac{T_{sep}}{L_T}$. For the values of table 1, this leads to $T_{sep} = 70$ eV and $E_r(1) = 3.9$ kV/m. The other E_r value is chosen at a fixed inner radial location. This means that the shear is modified by the two radial location values and not by a modified radial extension. The inner location is chosen to be $\rho = 0.97$ with E_r is estimated as follows: $E_r = \frac{\nabla P}{n} + V_\phi B_\theta - V_\theta B_\phi$. The toroidal velocity, V_ϕ, term will be neglected. For the determination of the poloidal velocity, V_θ, the neoclassical theory is used. In the edge region, ν^* varies strongly, therefore it is essential to model properly the transition from the banana, plateau and Pfirsch-Schlutter regimes. This is done thanks to the analytical formulation : $V_\theta = K_{neo}\frac{1}{B_\phi Z_i}\nabla T_i$ with K_{neo} from [17]. From the two E_r values, at the LCFS and at $\rho = 0.97$, a shearing rate is derived such that:

$$\gamma_E = \frac{\nabla E_r}{B} = \frac{E_r(0.97) - E_r(1)}{0.03 \times a \times B} \tag{3}$$

4. PARAMETRIC DEPENDENCIES OF THE RATIO BETWEEN THE MEAN FIELD TIME SCALE AND THE TURBULENCE TIME SCALE: γ_{turb}/γ_E

The impact of increasing the temperature on γ_{turb}, γ_E and their ratio is illustrated on figure 3, in the case where B is varied at fixed q. As T increases, γ_{turb} goes from RBM to ITG-TEM dominated regime as illustrated by the top panel of figure 3. B impacts γ_{turb} through α. γ_E increases with T and is weaker for larger B as seen on the middle panel of figure 3. Therefore a given value of γ_{turb}/γ_E is reached for larger T as B increases, see bottom panel of figure 3. If the temperature threshold is defined as the temperature above which γ_{turb}/γ_E is smaller than a given value, then one finds that T_{th} increases with larger B for any critical value of γ_{turb}/γ_E as illustrated by figure 4. This trend explains the robust almost linear scaling of the power threshold P_{th} with $n \times B \times S$ [1,2,3]. Indeed, if the core turbulence dominates in the edge region, then the power through a given surface can be expressed as $\frac{P_{th}}{S} \propto nT_{th}V_\perp$, with $V_\perp$ the velocity across the surface S [1]. Due to the γ_E dependence on $1/B$ equation 3, $T_{th} \propto B$ and hence $P_{th} \propto nBSV_\perp$.

At low density, a roll-over of the dependence on density is reported in most machines. The low density branch is associated with increased electron T_{th} as the density decreases. On the contrary, on the high density branch, T_{th} increases very weakly with increasing density [9,10,18]. In the turbulence model, increasing the density leads to larger collisionality, hence more unstable RBM for low temperatures. The $E \times B$ shearing is not affected by a modified density at these lower temperatures. For larger temperatures, associated with the low density branch, the

ITG-TEM branch takes over and is stabilized by larger densities. On the other hand, at higher T, the γ_E is increased with larger densities. This leads to two opposite trends: below 50-100 eV, a higher density leads to lower T_{th}, above 50-100 eV, a higher density leads to a weakly increasing T_{th}, as observed for the ratio of $\gamma_{turb}/\gamma_E = 0.15$ illustrated on figure 5. This trend is in agreement with experimental observations [9,10,18]. Nonetheless the modeled T_{th} is sensitive to the arbitrary choice of the critical value of γ_{turb}/γ_E below which one enters in H mode.
Recently, in JET-ILW, the ITPA 2004 scaling law including a Z_{eff} dependence [2] has been shown to reconcile better JET-C and JET-ILW observations. In the model, a higher Z_{eff} destabilizes the RBM branch, due to larger collisionality and stabilizes the ITG-TEM due to dilution and collisionality impacts. Concerning the $E \times B$ shear, modifying Z_{eff} impacts V_θ contribution to E_r, the dilution also modifies the pressure gradient term. At lower temperatures, γ_E is not affected by an increased Z_{eff}. At higher temperatures, γ_E is larger for larger Z_{eff}, hence the γ_E dependence on Z_{eff} could not explain the observed trend of a larger power threshold for larger Z_{eff}. Overall, at low temperatures, a lower temperature threshold due to lower Z_{eff} is due to reduced RBM growth. For $\gamma_{turb}/\gamma_E = 0.15$ and for two values of Z_{eff}, 2.2 and 1.3, respectively in the range found in JET-C and JET-ILW, the temperature threshold versus density exhibits a shift of its minimum towards lower values for higher Z_{eff}, see figure 6. Such a shift is consistent with the fact that in JET-ILW, at lower Z_{eff} the minimum in density has reappeared whereas in the same divertor configuration but with the C wall this minimum was not in the range experimentally explored [9].
A higher power threshold in H compared to D has been reported in various machine [1]. It was also reported that the temperature threshold itself depended on A_i [19]. At fixed $k_\theta \rho_i$, as it has been chosen here, the interchange growth rate scales as $1/\sqrt{A_i}$. A_i has no impact on the $E \times B$ shearing rate in the case where the potential at the LCFS is set by adiabaticity (if the potential is set by the sheath, then larger A_i will lead to higher E_r at the LCFS, hence greater $E \times B$ shear). The temperature threshold obtained for $\gamma_{turb}/\gamma_E = 0.15$ when changing the main ion from D to H is largely increased as illustrated on figure 7.

5. DISCUSSION

The approach proposed here is based on robust physical ideas: the turbulence and $E \times B$ interplay on the one hand and the stabilization of RBM on the other hand. The growth rate of the turbulent contribution derived analytically, for RBM and ITG-TEM, is shown to reproduce closely the main trends of a complete linear gyrokinetic simulation. The mean flow shear is based on two values. The E_r value at a inner location accounts for the fact that the collisionality regime is changing rapidly in this region, hence accounts for a poloidal velocity which merges the various collisional regimes. This approach can then robustly produce a temperature threshold as experimentally reported in [4,9,18,19,20,21] and explain various parametric dependencies such as a T_{th} increase with B, larger T_{th} for densities below the minimum in density while being weakly affected above the minimum, an upward shift of the minimum in density with reduced Z_{eff} and a higher T_{th} in H than in D.
Nonetheless, the main approximations of this approach are subject to discussion. The turbulence is assumed to scale with the main ion Larmor radius. The E_r shear is assumed to scale with the minor radius. The density and the temperature profiles are assumed to have unchanged gradient lengths. The toroidal rotation contribution in E_r is neglected. The role of a residual stress generating additional perpendicular rotation on E_r is not taken into account here. Since dithering L-H transitions are observed [22,23,24] and proposed to be explained by an inter-

play with the zonal and the mean flows [22,23], a shearing production rate scaling as $\sqrt{\gamma_{turb}\gamma_E}$ rather than γ_E could be tested. Finally, only a local variable such as T_{th} can be derived from this approach. Going from the derived T_{th} trends to P_{th} parametric dependencies is not straightforward.
Nevertheless, it is interesting to note that the ingredients of the model (namely: RBM and E_r using $V_\theta(\nu^*)$) are included in a flux driven fluid non-linear modeling which has recently demonstrated its ability to obtain an edge transport barrier when the power is increased [25]. These flux driven fluid simulations should now include ITG-TEM as well and study the parametric dependencies of the power threshold.

ACKNOWLEDGMENTS

This work was supported by EURATOM and carried out within the frame- work of the European Fusion Development Agreement. The views and opinions expressed herein do not necessarily reflect those of the European Commission.

REFERENCES

[1]. F. Ryter et al, Nuclear Fusion, **36**(9), 1217, 1996.
[2]. T Takizuka et al, Plasma Physics and Controlled Fusion, **46**(5A), A227, 2004.
[3]. Y R Martin eta l, Journal of Physics, **123**(1), 012033, 2008.
[4]. A J Meakins, et al, Plasma Physics and Controlled Fusion, **52**(7):075005, 2010.
[5]. J. W. Connor and H. R. Wilson. Plasma Physics and Controlled Fusion, **42**(1), R1, 2000.
[6]. B. N. Rogers and J. F. Drake. Physical Review Letters, **79**(2),229, 1997.
[7]. KH Burrell. Physics of Plasmas, **4**(5, 2), 1499, 1997.
[8]. C. Bourdelle, et al. Nuclear Fusion, **54**(2),022001, 2014.
[9]. C. F. Maggi et al. Nuclear Fusion, **54**,023007, 2014.
[10]. P. Sauter,et al. Nuclear Fusion, **52**(1):012001, 2012.
[11]. R. Neu et al. Journal of Nuclear Materials, **438**, S34, 2013.
[12]. F. Jenko. Computer Physics Communications, **125**(1-3):196.209, 2000.
[13]. C Bourdelle, et al. Plasma Physics and Controlled Fusion, **54**(11):115003, 2012.
[14]. P Cottier, et al. Plasma Physics and Controlled Fusion, **56**(1):015011, 2014.
[15]. M. Romanelli, et al. Plasma Physics and Controlled Fusion, **49**(6):935.946, 2007.
[16]. J. Loizu, et al. Plasma Physics and Controlled Fusion, **55**(12, 1-2), 2013.
[17]. F. L. Hinton and R. D. Hazeltine. Reviews of Modern Physics, **48**:239.308, 1976.
[18]. Y. Ma, et al. Nuclear Fusion, **52**(2):023010, 2012.
[19]. E Righi, et al. Plasma Physics and Controlled Fusion, **42**(5A):A199, 2000.
[20]. A. E. Hubbard, et al. Plasma Physics and Controlled Fusion, **40**(5):689.692, 1998.
[21]. W Suttrop, et al. Plasma Physics and Controlled Fusion, **39**(12):2051.2066, 1997.
[22]. L. Schmitz, et al. Physical Review Letters, **108**:155002, 2012.
[23]. G.R. Tynan, et al. Nuclear Fusion, **53**(7):073053, 2013.
[24]. T. Kobayashi, et al. Physical Review Letters, **111**:035002, 2013.
[25]. L. Chôné, et al. Physics of Plasmas, **21**(7):070702, 2014.

pulse	ρ	R/L_T	R/L_n	T	n	ν^*	q	s	Z_{eff}	B
82228	0.97	55	9	122	2.6	9.2	3.8	4.3	1.3	1.8

Table 1: Edge parameters for JET-ILW discharge 82228 prior to the L to H transition. The temperature is given in eV, the density n in $10^{19} m^{-3}$ and the magnetic field B in T.

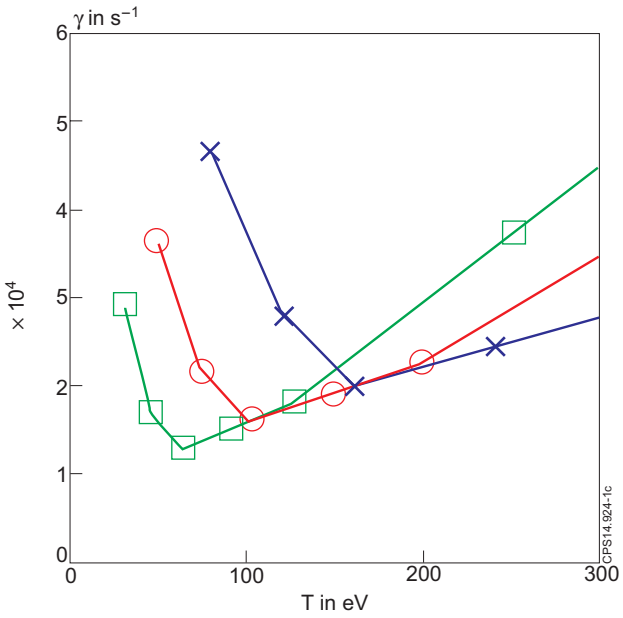

Figure 1: Growth rate computed by GENE at $k_\theta \rho_i = 0.1$ of the most unstable mode versus the temperature for the parameters of table 1.

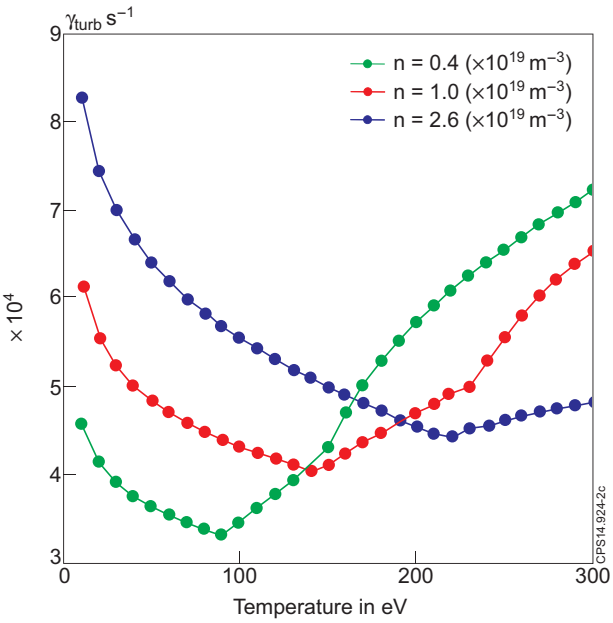

Figure 2: Growth rate in the fluid limit at $k_\theta \rho_i = 0.1$ versus the temperature for the parameters of table 1.

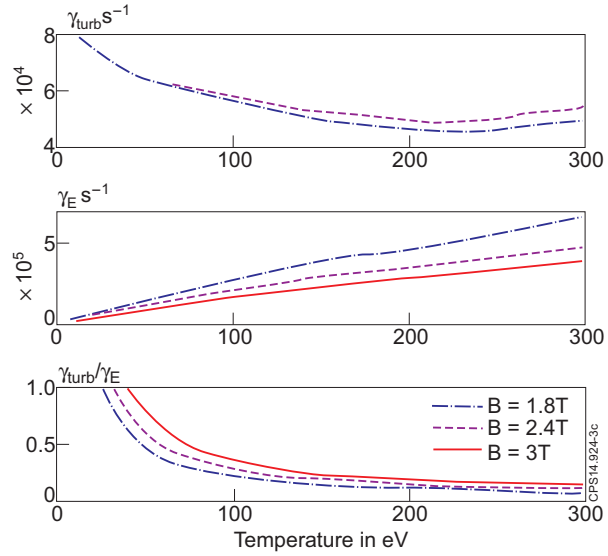

Figure 3: Top figure: turbulent growth rate γ_{turb} in s^{-1} as a function of temperature in eV for three values of the magnetic field at fixed q; middle figure: mean flow shearing rate γ_E in s_{-1} ; bottom figure, the ratio of γ_{turb}/γ_E.

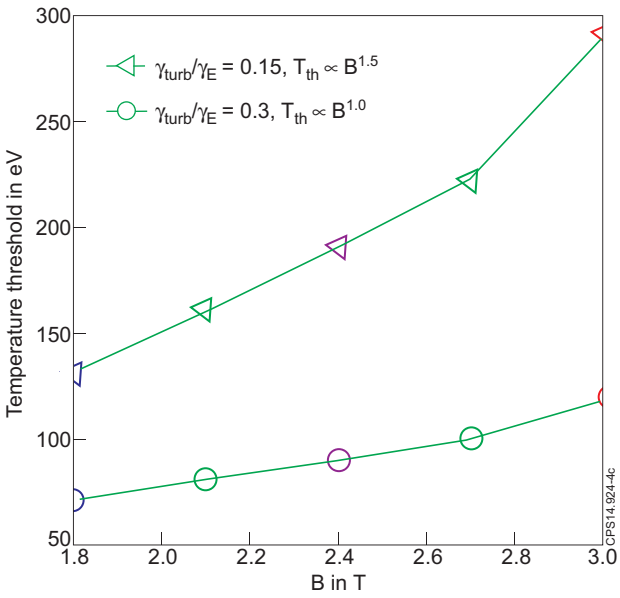

Figure 4: Temperature threshold versus magnetic field, at q fixed, for two values of γ_{turb}/γ_E. For B = 1.8T , 2.4T and 3T , the values are respectively signaled by the same colors used in figure 3, the other parameters are as reported in 1.

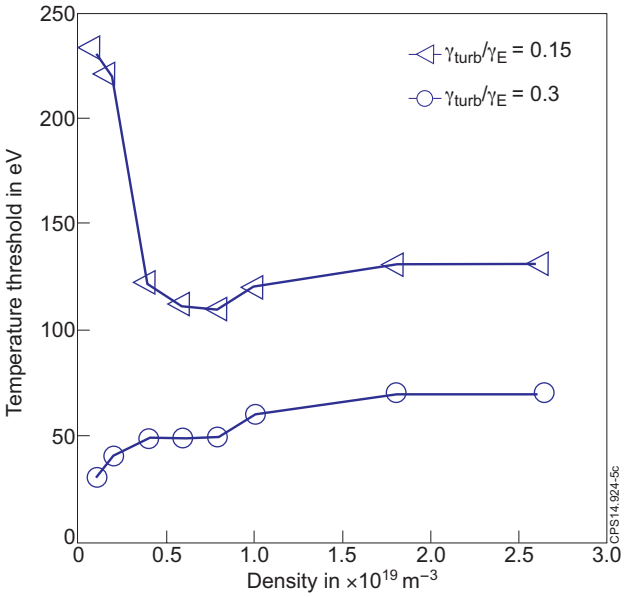

Figure 5: Temperature threshold versus density, for two values of γ_{turb}/γ_E, other parameters from table 1.

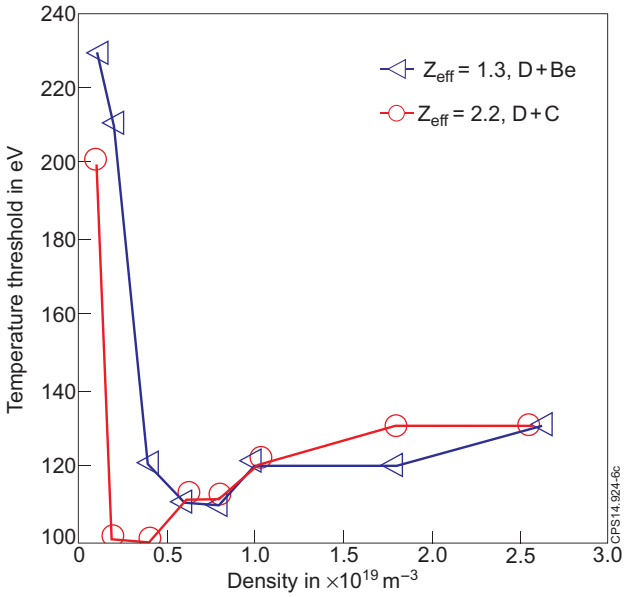

Figure 6: Temperature threshold versus density, for Z_{eff} = 1.3 and Z_{eff} = 2.2, other parameters from table 1 and γ_{turb}/γ_E = 0.15.

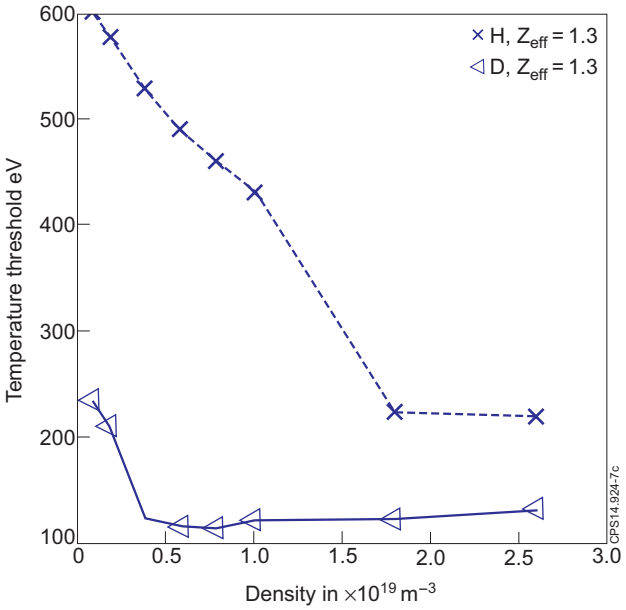

Figure 7: Temperature threshold versus density, for D and H, other parameters from table 1 and γ_{turb}/γ_E = 0.15.